



Department of Energy

Washington, DC 20585

QA: N/A

DOCKET NUMBER 63-001

August 19, 2009

ATTN: Document Control Desk

Christian Jacobs, Senior Project Manager
Project Management Branch Section B
Division of High-Level Waste Repository Safety
Office of Nuclear Material Safety and Safeguards
U.S. Nuclear Regulatory Commission
EBB-2B2
11545 Rockville Pike
Rockville, MD 20852-2738

**YUCCA MOUNTAIN – REQUEST FOR ADDITIONAL INFORMATION – VOLUME 2,
CHAPTER 2.1.1.4, SET 2 (DEPARTMENT OF ENERGY’S SAFETY ANALYSIS REPORT
SECTION 1.7) – Identification of Event Sequences**

Reference: Ltr, Jacobs to Williams, dtd 06/03/09, “Yucca Mountain - Request For Additional Information – Volume 2, Chapter 2.1.1.4, Set 2 & Set 3 (Department of Energy’s Safety Analysis Report Section 1.7)”

The purpose of this letter is to transmit two U.S. Department of Energy (DOE) responses to Request for Additional Information (RAI) Numbers 2 and 4 of Set 2 of the above-referenced letter. This set pertains to passive structure, system and component reliability. DOE has previously responded to RAI Number 1 of this set on June 9, 2009, RAI Number 5 on July 7, 2009, RAI Numbers 9, 10, 12 and 13 on July 14, 2009, RAI Numbers 7 and 8 on July 22, 2009, and RAI Numbers 3, 6, and 11 on August 5, 2009. This submittal completes the responses to the Set 2 RAIs of the above-referenced letter.

Each RAI response is provided as a separate enclosure. The DOE references cited in the responses, which have not been previously provided to the U.S. Nuclear Regulatory Commission, will be provided under separate cover.

There are no commitments in the enclosed RAI response. If you have any questions regarding this letter, please contact me at (202) 586-9620, or by email to jeff.williams@rw.doe.gov.

Jeffrey R. Williams, Supervisor
Licensing Interactions Branch
Regulatory Affairs Division
Office of Technical Management

OTM: SEG-1006



Printed with soy ink on recycled paper

Enclosures (2):

1. Response to RAI, Volume 2, Chapter 2.1.1.4, Set 2, Number 2
2. Response to RAI, Volume 2, Chapter 2.1.1.4, Set 2, Number 4

cc w/encls:

J. C. Chen, NRC, Rockville, MD
J. R. Cuadrado, NRC, Rockville, MD
J. R. Davis, NRC, Rockville, MD
R. K. Johnson, NRC, Rockville, MD
A. S. Mohseni, NRC, Rockville, MD
N. K. Stablein, NRC, Rockville, MD
D. B. Spitzberg, NRC, Arlington, TX
J. D. Parrott, NRC, Las Vegas, NV
L. M. Willoughby, NRC, Las Vegas, NV
Jack Sulima, NRC, Rockville, MD
Christian Jacobs, NRC, Rockville, MD
Lola Gomez, NRC, Rockville, MD
W. C. Patrick, CNWRA, San Antonio, TX
Budhi Sagar, CNWRA, San Antonio, TX
Bob Brient, CNWRA, San Antonio, TX
Rod McCullum, NEI, Washington, DC
B. J. Garrick, NWTRB, Arlington, VA
Bruce Breslow, State of Nevada, Carson City, NV
Alan Kalt, Churchill County, Fallon, NV
Irene Navis, Clark County, Las Vegas, NV
Ed Mueller, Esmeralda County, Goldfield, NV
Ron Damele, Eureka County, Eureka, NV
Alisa Lembke, Inyo County, Independence, CA
Chuck Chapin, Lander County, Battle Mountain, NV
Connie Simkins, Lincoln County, Pioche, NV
Linda Mathias, Mineral County, Hawthorne, NV
Darrell Lacy, Nye County, Pahrump, NV
Jeff VanNeil, Nye County, Pahrump, NV
Joe Kennedy, Timbisha Shoshone Tribe, Death Valley, CA
Mike Simon, White Pine County, Ely, NV
K. W. Bell, California Energy Commission, Sacramento, CA
Barbara Byron, California Energy Commission, Sacramento, CA
Susan Durbin, California Attorney General's Office, Sacramento, CA
Charles Fitzpatrick, Egan, Fitzpatrick, Malsch, PLLC

EIE Document Components:

001_NRC_Trans_Ltr_2.2.1.1.4_Set_2_No_5.pdf

002_Encl_2_4_2.2.1.1.4_Set_2.pdf

2,426 kB

RAI Volume 2, Chapter 2.1.1.4, Second Set, Number 2:

Provide technical bases for weighting factors used to develop the weldment fragility curves for canisters (SAR Section 1.7, BSC 2008a Section 6.3.7.4), and provide the weldment fragility curves.

In Section 6.3.7.4 of BSC, 2008a, the applicant has discussed the development of the weldment fragility curves for representative canisters. However, the applicant has not provided the weldment fragility curves, nor the technical bases for the weighting factors used to develop the curves.

1. RESPONSE

As discussed during the NRC clarification call of June 11, 2009, the DOE stated that the weldment fragility weighting factors described in *Seismic and Structural Container Analyses for the PCSA* (BSC 2008, Section 6.3.7.4) are not used to evaluate representative canister failure probabilities. The DOE agreed to explain the acceptability of the container analysis (BSC 2008) and NRC staff agreed that the weldment fragility curves do not need to be provided. The canister weldment regions are assigned the same material properties as the canister base material (BSC 2008, Table 6.3.3-2). This approach is consistent with assumptions used in similar analyses of structural challenges for DOE spent nuclear fuel canisters and multi-canister overpacks (MCOs) (Snow 2007, Sections 6.1.1, 6.2.1, and 6.3.1). The representative canister structural analysis provides a reasonable representation of the probability of canister failure without specific consideration of weldment fragility.

The purpose of the representative structural canister analyses is to establish reasonable reliability limits and provide confidence that, once canister-specific confirmatory structural analyses have been performed on canister designs that include tolerances for as-built variations in the canister, the preclosure safety analysis (PCSA) conclusions will remain valid. As discussed in SAR Section 5.10.2, the DOE will implement administrative controls to ensure that the reliability limits used in the PCSA are met. More specifically, SAR Table 5.10-3 establishes the canister and transportation cask acceptance program and identifies it as a probable subject of the license specifications. The DOE will establish and implement a program for the evaluation and acceptance of spent nuclear fuel and high-level radioactive waste shipping and storage canisters, and transportation casks prior to receipt at the repository.

CONSERVATISMS IN FRAGILITY CURVE

There are several unquantified yet conservative modeling techniques used in the development of the fragility curve for the representative canister. The use of tensile elongation data is more conservative than the use of compressive strain data for determining structural fragility under both tensile and compressive strain conditions. The fragility curve is adjusted to be consistent with code minimum values. The fragility curve does not account for the effects of localized plastic deformation or strain rate. In using the fragility curve, a maximum triaxiality factor of 2 is used regardless of the stress state.

The fragility curve used to evaluate the probability of failure for the canister material (BSC 2008, Table 6.3.7.3-1) is based on a statistical characterization of true strain at ambient temperature from 204 specimens of Stainless Steel Type 304 tubing obtained from slow strain rate tests. Data for Stainless Steel Type 304 bars and Stainless Steel Type 301 sheets/strips were found to have greater total elongations than the Stainless Steel Type 304 tubing data used (BSC 2008, Section 6.3.7.3). The use of tensile elongation data is more conservative than the use of compressive strain data for determining structural fragility under both tensile and compressive strain conditions. Furthermore, the Stainless Steel Type 304 tubing data are adjusted (engineering strain decreased by 8.3%) based on specifications which indicate that the minimum engineering strain for Stainless Steel Type 304 should be 35% (ASME 2006, p. 346) as opposed to 43.3% (obtained from the Stainless Steel Type 304 tubing data) and should correspond to a failure probability of 1% (BSC 2008, Section 6.3.7.3). This adjustment accounts for variability due to different steels used in typical canister designs.

The engineering strain (S) determined from the tensile elongation data is converted to true strain (ε) using the relation $\varepsilon = \ln(S+1)$ (BSC 2008, Section 6.3.7.3). This relation does not account for the effect of localized plastic deformation (necking) that occurs before tensile failure (i.e., it assumes that the entire volume of the specimen is in the same state of strain until failure). Tensile specimens experience localized plastic deformation such that the true strain in the necked region just prior to failure is larger than the strain obtained using this relation. Thus, the true strains at failure used to generate the fragility curves are underestimated.

As discussed in the response to RAI 2.2.1.1.4-2-004, the fragility curves are not adjusted for the effects of strain rate. Increased strain rate has a beneficial effect on material capability by increasing the amount of energy per unit volume required to achieve a given strain. Standardized DOE spent nuclear fuel canister and MCO drop analyses (Morton et al. 2002; Snow 2003; Snow 2007) make use of a material model in which the stress to achieve a given strain is increased by 20% relative to the quasi-static loading case. This material model resulted in agreement between calculated and measured deformation patterns and was reported to yield conservative simulation results (Morton et al. 2002, Part II, Sections 3.2.1 and 7.2). Therefore, not adjusting the representative canister material model for the effects of strain rate likely yields a conservative assessment of canister failure probabilities.

In evaluating the probability of canister failure using the fragility curves, triaxial stress states are accounted for by multiplying the calculated maximum effective plastic strain by a maximum triaxiality factor of 2 (corresponding to a ductility ratio of 0.5) (BSC 2008, Section 6.3.7.5). The use of the maximum triaxiality factor is conservative when the actual triaxiality factor is lower (e.g., when the local state of stress is such that it enhances plastic flow resulting in an actual triaxiality factor less than unity or during compression). The use of the maximum triaxiality factor can increase the calculated probability of failure by several orders of magnitude. For example, for a calculated true strain of 10% the calculated probability of failure without the triaxiality factor is about 3.6×10^{-15} per drop and with the triaxiality factor, about 2.68×10^{-8} per drop (BSC 2008, Table 6.3.7.3-1).

Analyses of structural challenges for DOE spent nuclear fuel canisters use a strain limit of 48% as a structural failure criterion (Morton et al. 2002, Section 7.4) and the analyses of the MCO use

a minimum fracture strain level of 118% or minimum elongation of 47% as a structural failure criterion (Snow 2003, Table 2). The adjusted fragility curve used to evaluate the probability of failure for the representative canister material (BSC 2008, Table 6.3.7.3-1) predicts a 99% probability of canister failure at a true strain of 48% and a 100% probability of failure at true strains of 54% and greater, which would include a true strain of 118%, even without consideration of the triaxiality factor. This provides more evidence that the fragility curve used in *Seismic and Structural Container Analyses for the PCSA* (BSC 2008, Table 6.3.7.3-1) is a conservative failure criterion.

CONSERVATISMS IN CANISTER STRUCTURAL ANALYSIS APPROACH

There are three conservatisms in the canister structural analysis approach: failure is calculated based on the maximum effective plastic strain for a single element brick, a smaller shell thickness is used for the representative canister than typical dual-purpose and transportation, aging, and disposal canisters, and two limiting drop heights are used in the PCSA.

In the canister structural analysis approach, the probability of failure is calculated based on the maximum effective plastic strain for a single element brick (with the greatest strain in the canister) (BSC 2008, Section 4.3.3.2). Although the analysis provides a distribution of strain values through the thickness of the canister wall (i.e., the wall thickness is represented by multiple finite element layers), it is more conservative to use the maximum effective plastic strain value at a single finite element than the average of the values across the wall thickness.

The canister structural analysis uses a representative canister (BSC 2008, Section 4.3.3.3) with a smaller shell thickness than those of typical dual purpose canisters and transportation, aging, and disposal canisters. The results of a sensitivity study involving end drops with a 4-degree off-vertical orientation of canisters with various shell thicknesses (BSC 2008, Section 6.3.3.6), indicate that the maximum effective plastic strain decreases with increasing shell thickness. Code minimum yield strength and tensile (ultimate) strength values are used for the representative canister structural analyses (BSC 2008, Section 4.3.3.3). It is reasonable to expect that the material properties of the fabricated canisters will exceed these minimums. Additionally, the structural analyses model the canister contacting a rigid, unyielding surface, thereby maximizing the amount of damage due to the collision (BSC 2009, Section 7). Therefore, it is reasonable to conclude that the results of the representative canister structural analyses are conservative with respect to the calculation of the maximum effective plastic strain.

In the PCSA, event sequences are developed for canister drops from the normal operational height and for canister drops from heights above the normal operational height (BSC 2009, Section A4.9.1). Conservatively, canister drops from heights less than the normal operational height are considered to occur from the maximum normal operating height and canister drops from heights greater than the maximum normal operating height are considered to occur from the maximum attainable height (i.e., a two-blocking event). Additional conservatism is incorporated in the analysis by assigning a failure probability of 10^{-5} to canister drop events with a calculated failure probability less than 10^{-8} (BSC 2009, Section 7).

Given the conservatisms used in developing the fragility curve and in the PCSA approach, it is reasonable to conclude that the representative canister structural analysis is a reasonable representation of the probability of canister failure, despite the use of base metal material properties in the weldment region.

2. COMMITMENTS TO NRC

None.

3. DESCRIPTION OF PROPOSED LA CHANGE

None.

4. REFERENCES

ASME (American Society of Mechanical Engineers) 2006. "Ferrous Material Specification." Section II, Part A of *2004 ASME Boiler and Pressure Vessel Code (includes 2005 and 2006 Addenda)*. New York, New York: American Society of Mechanical Engineers. TIC: 256479.

BSC (Bechtel SAIC Company) 2008. *Seismic and Structural Container Analyses for the PCSA*. 000-PSA-MGR0-02100-000-00A. Las Vegas, Nevada: Bechtel SAIC Company, ACC: ENG.20080220.0003.

BSC 2009. *Canister Receipt and Closure Facility Reliability and Event Sequence Categorization Analysis*. 060-PSA-CR00-00200-000-00B. Las Vegas, Nevada: Bechtel SAIC Company. ACC: ENG.20090112.0004.

Morton, D.K. and Blandford, R.K. 2008. *Impact Tensile Testing of Stainless Steels at Various Temperatures*. EDF-NSNF-082, Rev. 0. Idaho Falls, Idaho: Idaho National Laboratory. ACC: MOL.20090310.0082.

Snow, S.D. 2003. *Analytical Evaluation of the MCO for Repository-Defined and Other Related Drop Events*. EDF-NSNF-029, Rev. 0. Idaho Falls, Idaho: U.S. Department of Energy, Idaho Operations Office. ACC: MOL.20040510.0105.

Snow, S.D. 2007. *Structural Analysis Results of the DOE SNF Canisters Subjected to the 23-Foot Vertical Repository Drop Event to Support Probabilistic Risk Evaluations*. EDF-NSNF-085, Rev. 0. Idaho Falls, Idaho: Idaho National Laboratory. ACC: MOL.20080206.0062.

RAI Volume 2, Chapter 2.1.1.4, Second Set, Number 4:

Clarify whether or not thermal and strain-rate effects on the strength of canister steel material are considered in development of probability of failures for canister steel, listed in Table 6.3.7.3-1 (BSC. 2008a).

In Table 6.3.7.3-1 (BSC 2008a), the applicant has provided information on probability of failures versus true strain for canister steel. However, it is not clear whether or not the applicant has considered the effects of both temperature and strain-rate in developing the fragility curves for the canister steel.

1. RESPONSE

The use of representative canister material properties and the corresponding fragility curve provide a reasonable estimate of the probability of canister failure without considering the thermal and strain rate effects. Increasing strain rates increase the energy absorption capacity of the canister material. Although increasing temperatures decrease the overall structural strength of the canister material, canister drop analyses show that the peak strain is decreased and the strain profile is not as localized as at lower temperatures.

The purpose of the representative structural canister analyses is to establish reasonable reliability limits and provide confidence that, once canister-specific confirmatory structural analyses have been performed on canister designs that include tolerances for as-built variations in the canister, the preclosure safety analysis conclusions will remain valid. As discussed in SAR Section 5.10.2, the DOE will implement administrative controls sufficient to ensure that the reliability limits used in the preclosure safety analyses are met. More specifically, SAR Table 5.10-3 establishes the canister and transportation cask acceptance program and identifies it as a probable subject of the license specifications. The DOE will establish and implement a program for the evaluation and acceptance of spent nuclear fuel (SNF) and high-level radioactive waste shipping and storage canisters and transportation casks prior to receipt at the repository.

1.1 TEMPERATURE AND STRAIN-RATE VALUES USED IN CANISTER DROP ANALYSES

As discussed in the response to RAI 2.2.1.1.4-2-002, the fragility curve used to evaluate the probability of failure for the canister material (BSC 2008, Table 6.3.7.3-1) is based on a statistical characterization of ambient temperature engineering failure strain (total elongation) data from 204 specimens of Stainless Steel Type 304 tubing obtained from slow strain rate tests. The fragility curve is not adjusted for the effects of strain rate or temperature. Data for Stainless Steel Type 304 bars and Stainless Steel Type 301 sheets/strips were found to have greater total elongations than the Stainless Steel Type 304 tubing data used (BSC 2008, Section 6.3.7.3). The use of tensile elongation data is more conservative than the use of compressive strain data for determining structural fragility under both tensile and compressive strain conditions. Moreover, the Stainless Steel Type 304 tubing data were adjusted (engineering strain decreased by 8.3%) based on specifications that suggest that the minimum engineering strain for Stainless Steel Type 304 should be 35% (ASME 2006, p. 346) as opposed to 43.3% (obtained from the Stainless Steel

Type 304 tubing data) and should correspond to a failure probability of 1% (BSC 2008, Section 6.3.7.3). This adjustment accounts for variability due to different steels used in typical canister designs.

The material properties of the structural components of the canisters and casks are evaluated at a fixed temperature of 100°F (BSC 2008, Section 3.2.3.3). The selected temperature is sufficiently close to ambient temperature that the use of ambient temperature fragility curves in the representative canister drop analyses is consistent. The representative canister structural material is Stainless Steel Type 304L (BSC 2008, Section 6.3.7.3). Stainless Steel Type 304L is an austenitic stainless steel very similar to Stainless Steel Type 304, with slightly lower carbon content and potentially slightly higher nickel content. Minimum yield strength and tensile strength requirements for Stainless Steel Type 304L (25 ksi and 70 ksi, respectively) are only slightly lower than for Stainless Steel Type 304 (30 ksi and 75 ksi, respectively) (ASTM SA-213/SA-213M 2009, Tables 2 and 5). Both materials have identical minimum elongation requirements. Based on these considerations, the structural performance of Stainless Steel Type 304L will be similar to Stainless Steel Type 304. The material constants for the representative canister analyzed are listed in Table 6.3.3-2 of *Seismic and Structural Container Analyses for the PCSA* (BSC 2008) and correspond to quasi-static values (i.e., the effect of strain rate was not included).

1.2 EFFECT OF STRAIN RATE ON MATERIAL PROPERTIES

Stress-strain curves for Stainless Steel Type 304L indicate that while the effect of increased strain rates is to shift the curve to higher values of stress for a given strain, the maximum elongation is also decreased (Albertini and Montagnani 1980, Figure 2). These are competing effects on material fragility because the area under the stress-strain curve represents the capability of a unit volume of the material to absorb mechanical energy through deformation (BSC 2007, Section 7.1.7.2.2).

Morton and Blandford (2008) studied the effect of temperature (at -20, room temperature, 300, and 600°F) and strain rate (at 5, 10, 22, and 25 per second) on the tensile properties of Stainless Steel Type 304L and Stainless Steel Type 316L. Stainless Steel Type 316L is an austenitic stainless steel very similar to Stainless Steel Type 304L, with slightly increased nickel, slightly decreased chromium, and added molybdenum. Minimum yield strength, tensile strength, and elongation requirements for Stainless Steel Type 316L are identical to those for Stainless Steel Type 304L (ASTM SA-213/SA-213M 2009, Tables 2 and 5). Based on these considerations, the structural performance of Stainless Steel Type 316L will be similar to Stainless Steel Type 304L. Morton and Blandford (2008, Section 7) determined that the effect of strain rate on the stress-strain curve for both Stainless Steel Type 304L and Stainless Steel Type 316L was adequately represented by a multiplicative scaling factor applied to the quasi-static stress values.

In Figure 1, two schematic true stress-strain curves are represented, one that does not account for strain-rate effects (the quasi-static curve) and another that represents the effect of strain rate as a multiplier (κ) on the quasi-static curve. The elastic region and the region beyond the uniform strain have been omitted from this figure. The elastic region is omitted because it has a small effect and the region beyond the uniform strain is omitted because a discussion of the non-

uniform strain region of the curve is not necessary for this schematic comparison. In Figure 1, ε_1 is the strain required to absorb a given amount of mechanical energy per unit volume (represented as A_1), and ε_2 is the strain required to absorb a given amount of mechanical energy per unit volume (represented as A_2) in the case where strain rate is considered. If $\kappa = 1$, then the two curves overlap and the area under the two curves is equal ($A_1 = A_2$ and $\varepsilon_1 = \varepsilon_2$). If $\kappa > 1$, then, for a given strain, a greater amount of energy per unit volume would be absorbed at the higher strain rate. Morton and Blandford (2008, Section 7.2, Table 27) found that $\kappa > 1$ at all temperatures and strain rates evaluated. The value of κ increased as strain rate increased and also increased as temperature decreased. Therefore, at all temperatures evaluated, the energy absorption capacity of Stainless Steel Type 304L increases at increasing strain rates.

Finite element canister drop analyses of the standardized DOE SNF canister and multi-canister overpack (e.g., Morton et al. 2002 and Snow 2003) use a strain rate adjustment factor of $\kappa = 1.2$. This model resulted in adequate agreement between calculated and measured deformation patterns for drop tests of 18-inch DOE SNF canisters (Morton et al. 2002, Section 7.2). Overall, use of this material model yielded conservative simulation results (Morton et al. 2002, Section 3.2.1). Therefore, it is reasonable to conclude that not adjusting the material models for the effects of strain rate likely yields a conservative assessment of representative canister failure probabilities. Based on this observation, the use of representative canister material properties and the corresponding fragility curve, which are not adjusted for strain rate effects, is expected to provide a reasonable estimate of the probability of canister failure.

1.3 EFFECT OF TEMPERATURE ON MATERIAL PROPERTIES

Stress-strain curves for Stainless Steel Type 304L indicate that both ultimate tensile strength and uniform strain limit decrease with increasing temperatures above room temperature (Albertini and Montagnani 1980, Figures 2 and 5; Morton and Blandford 2008, Figure 31), suggesting lower material capability at higher temperatures. The increased ductility of Stainless Steel Type 304L at higher temperatures results in a greater volume of deformed material at lower applied stress values and a greater distribution of the load to adjacent portions of the canister. While essentially the same amount of mechanical energy is absorbed by the canister as a result of a drop at either temperature, the consumption of material capability is lower in the immediate vicinity of the peak equivalent plastic strain at higher temperatures. The results for a canister drop simulation at 70°F are shown in Figure 2 (Snow 2003, Figure 37), while those for a canister drop simulation at 240°F are shown in Figure 3 (Snow 2007, Figure 56). Figure 3 (240°F) shows elevated equivalent plastic strains for a much larger region of the canister shell than does Figure 2 (70°F). In Figure 3 (240°F), plastic strains greater than about one-half of the peak equivalent plastic strain value, of approximately 4%, correspond with the green shaded areas and extend well away from the peak equivalent plastic strain location. At 70°F (Figure 2), the green shaded areas that are characteristic of about one-half the peak equivalent plastic strain value, approximately 17%, are localized closer to the location of the peak equivalent plastic strain.

Based on the above discussion, the use of representative canister material properties and the corresponding fragility curve, which are not adjusted for temperature and strain rate effects, provide a conservative but reasonable estimate of the probability of canister failure.

2. COMMITMENTS TO NRC

None.

3. DESCRIPTION OF PROPOSED LA CHANGE

None.

4. REFERENCES

Albertini, C. and Montagnani, M., 1980. "Dynamic Uniaxial and Biaxial Stress-Strain Relationships for Austenitic Stainless Steels." *Nuclear Engineering and Design*, 57, 107-123. TIC: 260372.

ASME (American Society of Mechanical Engineers) 2006. "Ferrous Material Specification." Section II, Part A of *2004 ASME Boiler and Pressure Vessel Code (includes 2005 and 2006 Addenda)*. New York, New York: American Society of Mechanical Engineers. TIC: 256479

ASTM (American Society for Testing and Materials) SA-213/SA-213M, 2009. *Specification for Seamless Ferritic and Austenitic Alloy-Steel Boiler, Superheater and Heat-Exchanger Tubes*. New York, New York: American Society of Mechanical Engineers.

BSC (Bechtel SAIC Company) 2007. *Waste Package Component Design Methodology Report*. 000-30R-WIS0-00100-000-004. Las Vegas, Nevada: Bechtel SAIC Company. ACC: ENG.20071220.0030.

BSC 2008. *Seismic and Structural Container Analyses for the PCSA*. 000-PSA-MGR0-02100-000-00A. Las Vegas, Nevada: Bechtel SAIC Company, ACC: ENG.20080220.0003.

Morton, D.K.; Snow, S.D.; and Rahl, T.E. 2002. *FY1999 Drop Testing Report for the Standardized 18-Inch DOE SNF Canister*. EDF-NSNF-007, Rev. 2. Idaho Falls, Idaho: U.S. Department of Energy, Idaho Operations Office. ACC: MOL.20040510.0104.

Morton, D. K. and Blandford, R. K., 2008. *Impact Tensile Testing of Stainless Steels at Various Temperatures*. EDF-NSNF-082, Rev. 0. Idaho Falls, Idaho: Idaho National Laboratory. ACC: MOL.20090310.0082.

Snow, S.D. 2003. *Analytical Evaluation of the MCO for Repository-Defined and Other Related Drop Events*. EDF-NSNF-029, Rev. 0. Idaho Falls, Idaho: U.S. Department of Energy, Idaho Operations Office. ACC: MOL.20040510.0105.

Snow, S.D. 2007. *Structural Analysis Results of the DOE SNF Canisters Subjected to the 23-Foot Vertical Repository Drop Event to Support Probabilistic Risk Evaluations*. EDF-NSNF-085, Rev. 0. Idaho Falls, Idaho: Idaho National Laboratory. ACC: MOL.20080206.0062.

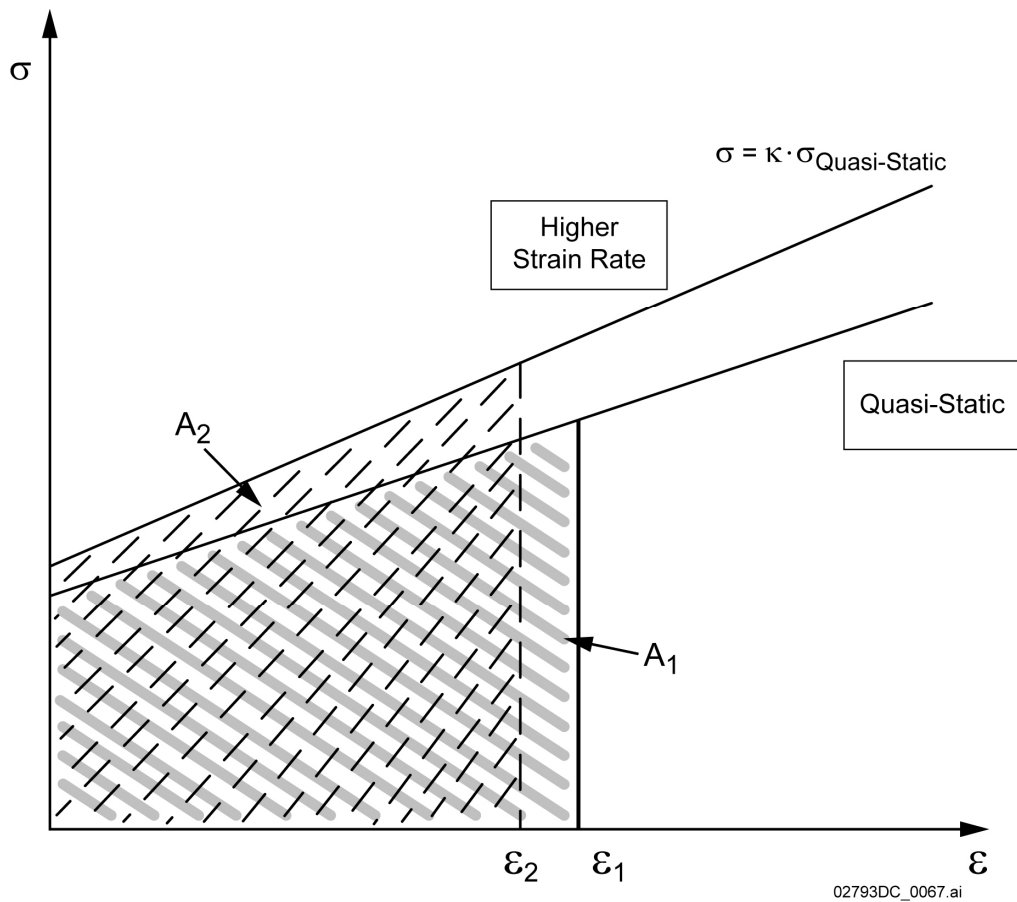


Figure 1 Stress-Strain Curves Illustrating the Effect of Strain-Rate

ENCLOSURE 2

Response Tracking Number: 00399-00-00

RAI: 2.2.1.1.4-2-004

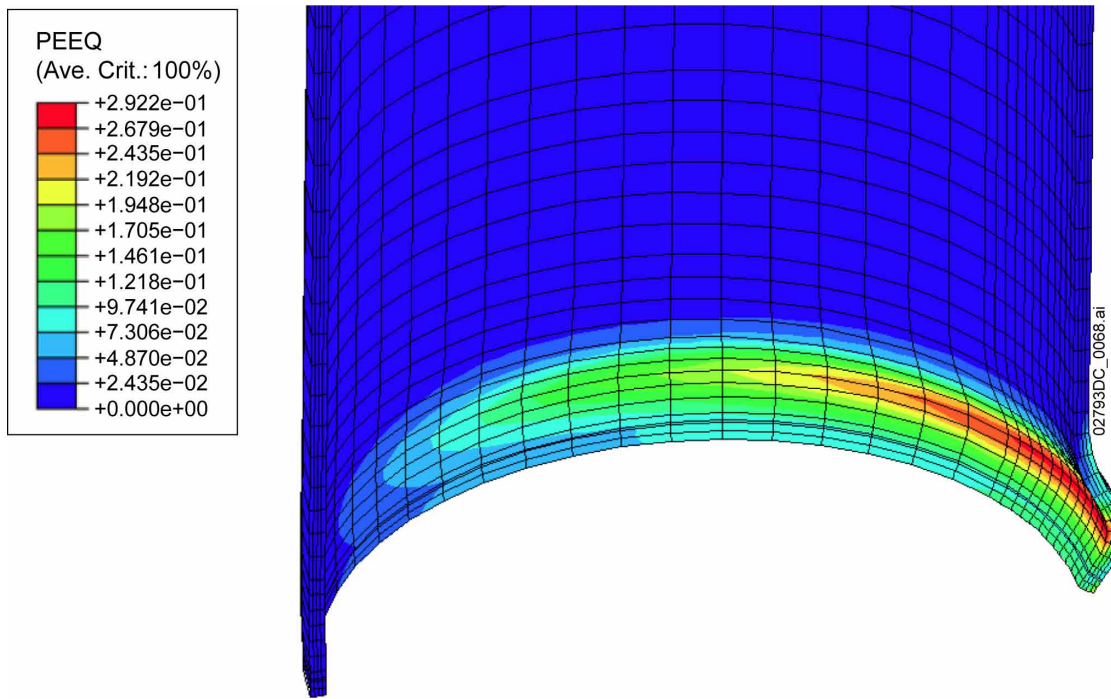


Figure 2. Multi-Canister Overpack Mark IV, 23-Foot 3 Deg. Off-Vertical Drop—Main Shell Strains—70°F

Source: Snow 2003, Figure 37

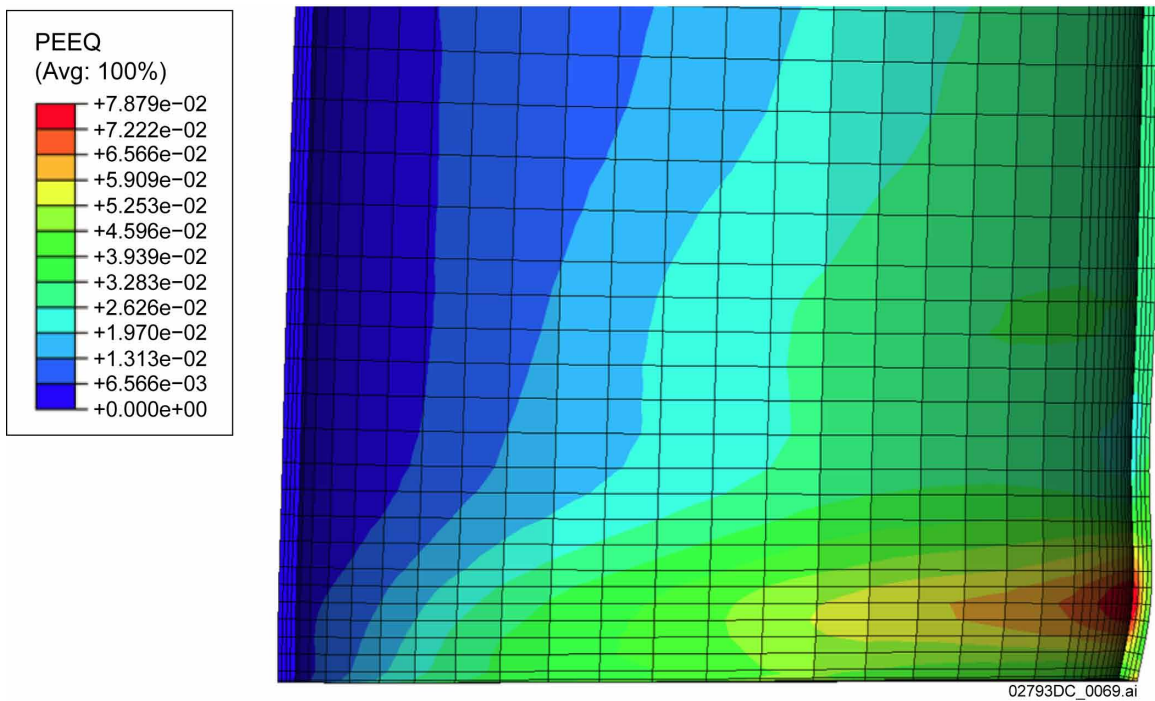


Figure 3. Multi-Canister Overpack Mark IV, 23-Foot 3 Deg. Off-Vertical Drop—Main Shell Strains—240°F

Source: Snow 2007, Figure 56